

FULLY AUTOMATED, HEXAHEDRAL MESHING OF PATIENT-SPECIFIC CARTILAGE STRUCTURES: DATA FROM THE OSTEOARTHRITIS INITIATIVE

Borja Rodriguez-Vila (1,2), David M. Pierce (3,4)

(1) Bioengineering and Telemedicine Centre
Universidad Politécnica de Madrid
Madrid, Spain

(3) Department of Mechanical Engineering
University of Connecticut
Storrs, CT, USA

(2) Networking Research on Bioengineering
Biomaterials and Nanomedicine (CIBER-BBN)
Madrid, Spain

(4) Department of Biomedical Engineering
University of Connecticut
Storrs, CT, USA

INTRODUCTION

Articular cartilage in diarthrodial joints must provide (i) a compliant, low-friction surface between the relatively rigid bones; (ii) a long-wearing and resilient surface; and (iii) a means to distribute the contact pressure to the underlying bone structure. Osteoarthritis (OA) is a disease of the synovial joint, with degeneration and loss of articular cartilage as one hallmark change. OA is a debilitating disease that afflicts nearly 20% of people in the US, costing more than \$185.5 billion a year (in 2007 dollars), and its prevalence is projected to increase by about 40% in the next 25 years [1,2].

Fortunately, we can access large cohort databases on the progression of OA, e.g. the Osteoarthritis Initiative (OAI), with a cohort of 4,796 participants. The OAI is a multicenter, longitudinal, observational study of knee OA funded in part by the NIH [5]. This study selects men and women from the general population who likely either have preexisting OA or are at high risk as indicated by weight, knee symptoms, or history of knee injuries. The OAI public database supports investigations of knee OA onset and progression using traditional measures of disease and biomarkers developed from the study. Additionally, 3.0 T Siemens Trio Magnetic Resonance Images (MRIs) are available, including: localizer (3-plane), intermediate-weighted turbo spin echo, 3-D dual-echo in steady-state (DESS), intermediate-weighted turbo spin echo, T1-weighted 3-D flash and T2.

Despite the multifactorial nature of OA, mechanical stresses play a key role in the destructive evolution of the disease [3,4]. Both overloading (e.g. trauma) and reduced loading (e.g. immobilization) of cartilage induce molecular and microstructural changes that lead to mechanical softening, fibrillation, and erosion. Experiments can be used to quantify mechanical properties and biology of tissues, and imaging can be used to estimate tissue structure and even strains; however, only

computational models can estimate intra-tissue stresses in human joints because the required *in vivo* experiments are impossible or unsafe. Finite element (FE) models are well-established at the macro (e.g. joint) scale as a means to estimate stress distributions.

Generating an appropriate computational mesh is prerequisite for applying many numerical techniques, including FE analyses, to patient-specific questions. Such meshes represent the geometry of interest using a set of polyhedral elements, commonly tetrahedra (a minimum of four connected nodes creating four triangular faces) or hexahedra (a minimum of eight connected nodes creating six quadrilateral faces). Many fast and robust methods exist for automatically generating tetrahedral meshes of arbitrary geometries, cf. [6,7].

Building computational meshes from hexahedra is far more restrictive, and a fully automatic algorithm for generating hexahedral meshes of arbitrary geometries has not yet been achieved. However, for a wide range of applications, hexahedral-based meshes are preferred. Among many reasons, FE meshes require far more tetrahedral elements (relative to hexahedral elements) to achieve the same solution accuracy for a given analyses, and this leads to higher computational costs (both time and memory) [8]. Additionally, when the aim is to apply FE analyses, tetrahedral meshes produce acceptable displacement results but are relatively inaccurate for predicting stresses [9].

In this work we propose a specific algorithm designed to work with patient-specific geometries of the knee obtained from MRI. Indeed, we establish a fully automated methodology for hexahedral meshing of knee joint structures, i.e. femoral cartilage, tibial plateau and menisci.

METHODS

MRI data sets from the OAI include 160 slices of 384x384 pixels², for a final voxel resolution of 0.365x0.365x0.7 mm³. We label

anatomical structures of the knee in each patient by manually segmenting sagittal slices of the fat-suppressed 3D dual-echo in steady state (DESS) from the OAI database (**Figure 1a**). DESS appears to be the best sequence to capture quantitative cartilage morphometry and to provide the best universal cartilage discrimination. From the manual segmentations we generate triangular surfaces of each structure using a marching cubes algorithm (**Figure 1b**).

We start from triangular surfaces of the structures of interest as inputs to our fully automatic, hexahedral meshing methodology for knee joint structures, i.e. femoral cartilage, medial/lateral tibial plateau and medial/lateral menisci. Our methodology uses the minimum bounding box of each structure to perform specific and customized sweeping algorithms, and while minimizing the use of collapsed elements.

In every case, the process pipeline is similar: (1) generate a low-element-density model with a custom sweeping algorithm which takes into account the structure's geometry, (2) apply Laplacian smoothing, (3) refine the model by subdividing hexahedrons, (4) expand the model to fit the original (triangular surface) segmentation, (5) smooth the model to eliminate sharp borders, and (6) optimize the quality of the elements. The mesh density is fully adjustable and we form meshes for femoral and tibial cartilages using three different layers (superficial/middle深深) to allow use of different material parameters.

We demonstrate the quality of our patient-specific meshes of in the human knee using the element scaled Jacobian \hat{J} , a common quality metric for the analyses of solid structures [10]. Each hexahedral element has a center, $k = 0$, and nodes, $k \in [1, \dots, 8]$, as well as edges (e_{k1}, e_{k2}, e_{k3}) connected to each node. We evaluate the scaled Jacobian of an element as the minimum of each nodal Jacobian divided by the length of the three corresponding edges using

$$\hat{J} = \min_{k \in [0, \dots, 8]} \left[\frac{e_{k1} \cdot (e_{k2} \times e_{k3})}{\|e_{k1}\| \|e_{k2}\| \|e_{k3}\|} \right], \quad (1)$$

where the scaled Jacobian takes the range $[-1, 1]$ for a hexahedral element, with -1 corresponding to the worst possible elements and $+1$ the best possible ones (NB: only elements with a nonzero, positive scaled Jacobian are suitable for FE analysis [10]).

RESULTS

Using baseline MRIs from six patients in the OAI database we manually segmented the cartilages and menisci, reconstructed and smoothed them in 3-D, and individually meshed them with hexahedral FEs. In all cases our methodology obtains the patient-specific meshes of interest from the triangular surfaces in less than 4 minutes running a MATLAB implementation on a common PC (**Tables 1,2**). Scaled Jacobian values of the meshes range from 0.5 to 1, where $\sim 90\%$ of the elements have values >0.8 , and only 1.2% have values from 0.5 to 0.6.

Table 1: Mesh quality metrics ($M \pm SD$) by anatomical structure (Fem.=Femoral, Cart.=Cartilage, Tib.=Tibial, M.=Medial, L.=Lateral).

Structure	Elements (#)	Time (s)	$\hat{J} > 0.8$ (%)	$0.6 > \hat{J} > 0.5$ (%)
Fem. Cart.	24502 \pm 2758	80 \pm 7	94.67 \pm 0.93	0.96 \pm 0.14
M. Tib. C.	3816 \pm 0	11 \pm 1	93.27 \pm 3.74	0.24 \pm 0.30
L. Tib. C.	3906 \pm 0	11 \pm 1	94.62 \pm 2.04	0.14 \pm 0.09
M. Men.	1880 \pm 98	44 \pm 18	55.01 \pm 7.10	6.84 \pm 3.32
L. Men.	1700 \pm 34	57 \pm 21	42.89 \pm 2.55	11.33 \pm 1.6

Table 2: Mesh quality metrics organized by OAI patient ID [5].

OAI ID	Elements (#)	Time (s)	$\hat{J} > 0.8$ (%)	$0.6 > \hat{J} > 0.5$ (%)
9932809	37712	188	90.44	1.49
9948792	39562	221	89.29	1.51
9961728	37662	174	90.90	1.61
9977985	35366	226	90.40	1.25
9988421	31640	200	88.60	1.83
9988820	33482	226	90.38	1.82

The hexahedral meshes we obtained using our methodology (**Figure 1c**) correctly match the initial triangular surfaces (**Figure 1b**), with a RMS value (comparing the input triangular surfaces to the final hexahedral meshes) below 1 mm. We use collapsed elements in only the meshes of the femoral cartilages, resulting in a maximum of 12 wedges for an individual patient.

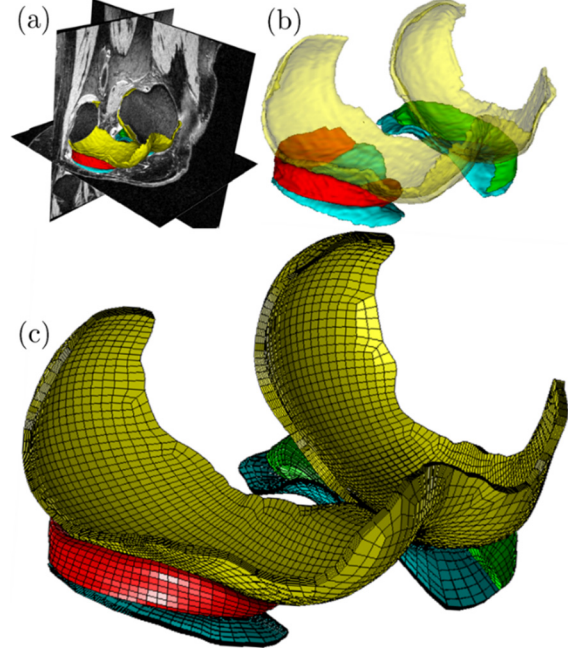


Figure 1: Representative patient-specific finite element (FE) mesh established from baseline magnetic resonance images (MRIs) from the OAI database. (a) Segmentation of cartilages and menisci. (b) 3-D reconstruction of femoral (yellow) and tibial (blue) cartilages, medial (green) and lateral (red) menisci. (c) Corresponding mesh of 20-node hexahedral FEs.

DISCUSSION

Our preliminary, fully hexahedral meshing methodology preserves tissue volume and produces high-quality elements. To the best of our knowledge, no other automatic hexahedral meshing for patient-specific knee structures has been proposed in the literature.

We hope to provide a fundamentally different means to test hypotheses on the mechanisms of disease progression at the patient level by integrating our patient-specific FE meshes and analysis framework, cf. [11], with data from individual patients or from natural history databases, e.g. the OAI. In the longer term, simulation-based, predictive medicine combined with medical imaging will likely improve the health, well-being, and quality of life for patients with OA.

REFERENCES

- [1] Lawrence, RC et al., *Arthritis Rheum*, 58:26-35, 2008.
- [2] Kotlarz, H et al., *Arthritis Rheum*, 60:3546-3553, 2009.
- [3] Goldring MB, Marcu KB, *Arthritis Res Ther*, 11:224, 2009.
- [4] Loeser, RF et al., *Arthritis Rheum*, 64:1697-1707, 2012.
- [5] Nevitt, M et al., *The OAI: Protocol for the Cohort Study*, 2006.
- [6] Löhner R, Parikh P, *Int J Num Method Fluids*, 8:1135-49, 1988.
- [7] Yerry MA, Shephard MS, *Int J Num Method Eng*, 20:1965-90, 1984.
- [8] Ramos A, Simões JA, *Med Eng Phys*, 28:916-924, 2006.
- [9] Puso MA, Solberg J, *Int J Num Methods Eng*, 67:841-867, 2006.
- [10] Tarjuelo-Gutierrez J et al., *Med Biol Eng Comp*, 52:159-168, 2014.
- [11] Pierce D et al., *Biomech Model Mechanobiol*, 15:229-244, 2016.